Uniaxial pressure effect on the magnetic phase diagram and Fermi-surface properties of CeB_6

T. Yamamizu, M. Endo, M. Nakayama, N. Kimura, and H. Aoki*
Center for Low Temperature Science, Tohoku University, Aramaki aza Aoba, Sendai 980-8578, Japan

S. Kunii
Graduate School of Science, Tohoku University, Aramaki aza Aoba, Sendai 980-8578, Japan
(Received 24 April 2003; revised manuscript received 28 July 2003; published 30 January 2004)

The magnetic phase diagram and the de Haas–van Alphen (dHvA) effect of CeB_6 have been studied under uniaxial pressures and magnetic fields applied parallel to [001]. Two phases IIA and IIB in the antiferroquadrupolar (AFQ) state and three phases III″, III, and III′ in the antiferromagnetic (AFM) state are found. With application of a small uniaxial pressure, the low-field phases IIA and III″ change drastically and are likely to disappear. On the other hand, the AFQ transition temperature for the high-field phase IIB does not change within experimental error. The AFM transition temperature for phase III, the transition field between phases III and III″, and the one between III″ and paramagnetic phases all increase with uniaxial pressure. The dHvA frequency increases with uniaxial pressure, whereas it is expected to decrease from the area change of the reciprocal space. The effective mass increases rapidly with uniaxial pressure at low pressures and then does not change appreciably at high pressures. The present observations of the uniaxial pressure effects are qualitatively different from those of hydrostatic pressure effects. By comparing the hydrostatic and uniaxial pressure effects, we argue that the compressions along the [001] direction and in the (001) plane give very different effects, reflecting the quadrupolar order.

DOI: 10.1103/PhysRevB.69.014423 PACS number(s): 75.30.Kz, 71.27.+a, 75.30.Mb, 71.18.+y

I. INTRODUCTION

CeB_6 has been most intensively studied as a typical compound which shows antiferroquadrupolar (AFQ) order. With decreasing temperature it exhibits AFQ transition at 3.3 K and then antiferromagnetic (AFM) transition at 2.4 K. It also shows a dense Kondo behavior. These interactions compete with each other to give rise to fascinating properties of this compound.

A pressure has been used as a powerful tool to change the relative strengths of the competing interactions. For example, according to the Doniach model,[1] the relative strength of the Ruderman-Kittel-Kasuya-Yosida (RKKY) and the Kondo effect can be tuned by pressure. It is also rather well understood how the Kondo effect or the RKKY interaction arises from the interaction between the *f* electron and the conduction electrons or how the electronic structures of the conduction electrons are affected by them. On the other hand, a few experimental studies have been performed for the pressure effect on the quadrupolar interaction or the quadrupolar order. Moreover, little is known about the microscopic mechanism of the quadrupolar interaction or how the quadrupole or the quadrupolar order affects the electronic structure of the conduction electron. To pursue these issues, it would be interesting and useful to clarify how the electronic structure as well as the physical properties associated with quadrupolar interaction change with pressure.

The hydrostatic pressure effects on quadrupolar transition temperature (T_Q) and AFM transition temperature (T_N) or on the phase diagram of CeB_6 have been studied by various groups.[2–5] The electronic structure changes with hydrostatic pressure has been studied by us[6] using the de Haas–van Alphen (dHvA) effect. On the other hand, there are few experimental studies on the uniaxial pressure effect, although a uniaxial pressure is an interesting tool to study the system with quadrupolar order. For example, the uniaxial pressure lowers the symmetry of the crystal and therefore affects the degenerate ground state from which the orbital degrees of freedom arise. Particularly, it can produce strain with a particular symmetry which couples with quadrupoles of the same symmetry and therefore would affect significantly the quadrupolar order and the properties closely related with it. In the previous papers we have investigated such effect of uniaxial pressure on the magnetic phase diagram and electronic structure of the system with quadrupolar order $Ce_3Pd_{20}Ge_6$.[7,8]

Another interesting effect of uniaxial pressure is to deform the sample quite differently from the hydrostatic pressure, i.e., it compresses the sample along the axis but expands the sample in the perpendicular plane to the axis. In the ordered state of quadrupoles the electronic structure as well as the physical properties must be anisotropic reflecting the order. The anisotropic *f* electron state due to the quadrupole order has been studied by resonant x-ray experiments.[9] However, it is difficult to see the anisotropy of the electronic structure of the conduction electrons and therefore few pieces of experimental evidence for such anisotropy have been reported. The anisotropy is also expected to be reflected in the pressure effect. However, hydrostatic pressure compresses the sample in all directions; it would be difficult to pick up a peculiar effect arising from the anisotropy. On the other hand, by comparing the effect of uniaxial pressure with that of hydrostatic pressure, the difference between the effects of compression along the axis and in the perpendicular plane could be investigated.

This paper reports the first systematic study of the uniaxial pressure effect on the phase diagram and the electronic structure of CeB_6. The dHvA effect and ac suscepti-

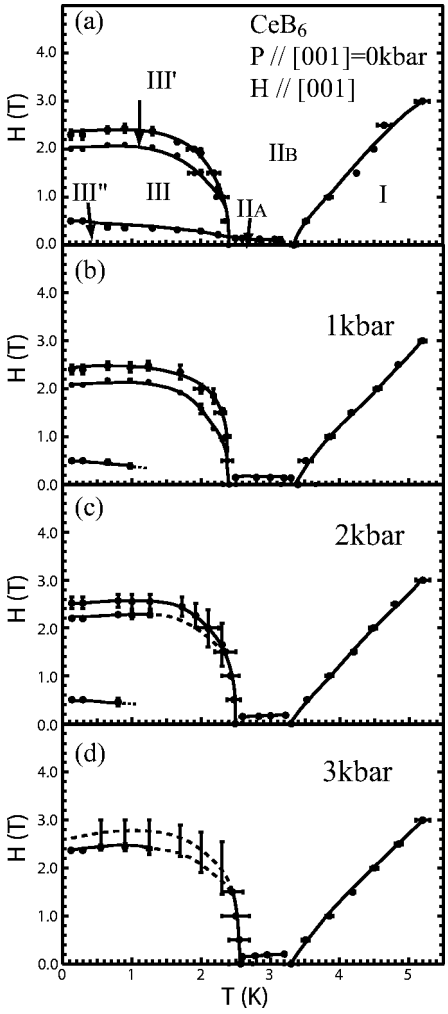

FIG. 1. Magnetic phase diagram of CeB_6 at pressures 0 kbar, 1 kbar, 2 kbar, and 3 kbar. The uniaxial pressure and magnetic field are applied parallel to [001]. The solid lines are guides to the eye.

bility are used to investigate the Fermi-surface properties and the magnetic phase diagram of CeB_6 under uniaxial pressures. We have found a qualitatively very different effect of uniaxial pressure from that of hydrostatic pressure. Particularly, a very drastic effect of uniaxial pressure has been found for the low-field phases.

Section II describes sample preparation and experimental procedures. Section III reports the magnetic phase diagram and the dHvA effect under uniaxial pressures. In Sec. IV we compare the magnetic phase diagram and the dHvA effect under uniaxial pressures with that under hydrostatic pressures. We pay a particular attention to the low-field phases in the AFQ and AFM states whose origins have not been clarified. Finally by analyzing the experimental results under uniaxial and hydrostatic pressures, we show that the present pressure effect is consistent with the symmetry of the quadrupolar order.

II. EXPERIMENTS

Single crystals of CeB_6 were grown by the floating method and cut into a rectangular shape of $2\times2\times4$ mm^3 with the long axis parallel to [001]. The two opposite (001) planes of the sample are carefully polished to be parallel to each other and to have smooth surfaces. Uniaxial pressures and magnetic fields were applied parallel to the [001] direction. A clamp-type cell with a spring inside is used to produce the uniaxial pressure. The pressure was applied at room temperature and the pressures at low temperatures were monitored by a strain gage to confirm that the pressure does not change more than 0.05 kbar at low temperatures. The dHvA effect was measured by using a dilution refrigerator in magnetic fields up to 15 T. The dHvA signal was detected by using the standard field modulation technique. The ac susceptibility measurements were performed using the same setting with that for the dHvA measurements in the dilution refrigerator or in a ^{3}He cryostat. We have chosen appropriate modulation field and frequency depending on the purpose of experiment so that the heating effect of the cell does not affect the measured quantities significantly.[10,11]

The phase-shift analysis was used to determine the frequency change with pressure. This method is very accurate to determine the small change of the frequency but cannot determine whether the frequency increases or decreases. Therefore, as a complementary method the fast Fourier transform (FFT) was also used at each pressure to determine the frequency semiquantitatively. The effective mass was determined both from the temperature dependence of the Fourier amplitude of the signal in the field range between 14 T and 14.7 T and the peak to peak amplitude of the dHvA oscillation at around 14.6 T. In this paper we conventionally use symbol H to denote the magnetic-flux density coming from externally applied field. Symbol B is used only when we need to take the effect of magnetization into account.

III. RESULTS

A. Magnetic phase diagram

Figure 1 shows the magnetic phase diagram determined by the ac susceptibility measurements under uniaxial pressures of 0 kbar, 1 kbar, 2 kbar, and 3 kbar. The magnetic phase diagram at 0 kbar is consistent with those reported previously by Nakamura *et al.*[12] and Brandt *et al.*[2] We denote the paramagnetic phase as phase I, and the two phases in the AFQ state as IIA and IIB, and the three phases in the antiferromagnetic state as III″, III, and III′ following the notation of Nakamura *et al.*[12] In the following we describe more details of the phase diagram and the related ac susceptibility measurements.

First we describe the ac susceptibility measurements at a constant magnetic field as a function of temperature to determine the antiferroquadrupolar transition temperature $T_Q(H)$ and the antiferromagnetic transition temperature $T_N(H)$. Figure 2 shows the ac susceptibility as a function of temperature at zero magnetic field or in phases I, IIA, and III″. At ambient pressure T_Q is defined by the inflection point of the curve and T_N by the peak of the curve. With application of pressure of 1 kbar, the curve form of the susceptibility qualitatively changes particularly below T_Q. This qualitative change is also demonstrated as a function of magnetic field later in Fig. 7. The change at T_Q becomes very weak, but still

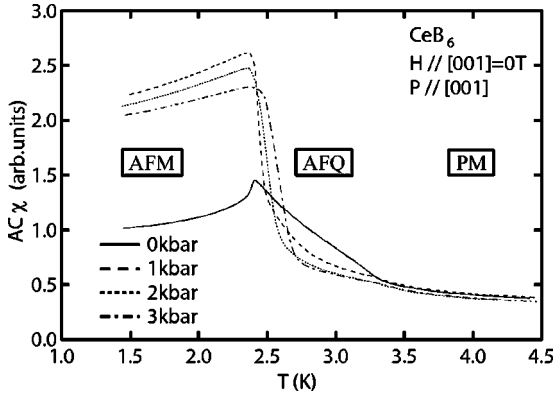

FIG. 2. ac susceptibility of CeB_6 at uniaxial pressures 0 kbar, 1 kbar, 2 kbar, and 3 kbar as a function of temperature under zero magnetic field. The uniaxial pressure is applied parallel to [001]. PM, AFQ, and AFM denote paramagnetic phase, antiferroquadrupolar phase, and antiferromagnetic phases, respectively. The positions where the letters are placed show approximately the temperature regions of the phases.

a very weak change can be observed there. We have temporarily plotted these temperatures as T_Q's under uniaxial pressure in Figs. 1(b)–1(d). However, the weak change could arise from an inhomogeneity of strain and may not correspond to the AFQ transition under uniaxial pressure. This point will be discussed in Sec. IV B. With decreasing temperature the susceptibility shows sharp increase at around 2.5 K, and then makes a peak at around 2.4 K. With further application of pressure up to 3 kbar, no qualitative change takes place in the behavior of the susceptibility curve. We have plotted the inflection point and the peak as the two ends of the error bar for the T_N under uniaxial pressures. Since the curve form changes between 0 kbar and 1 kbar, it is difficult to say whether T_N increases or decreases. However, if we compare the curve forms under uniaxial pressures, we can see that T_N increases with uniaxial pressure. This point is also discussed later in Sec. IV B.

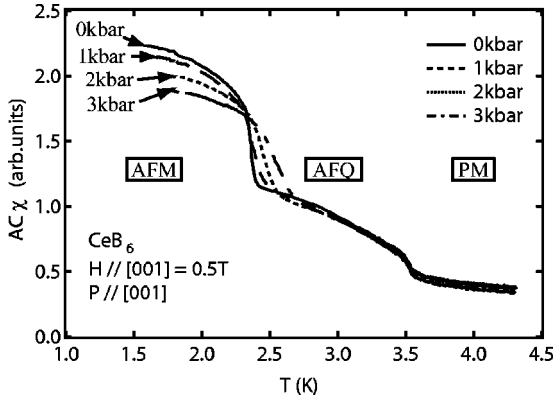

FIG. 3. ac susceptibility of CeB_6 at uniaxial pressures 0 kbar, 1 kbar, 2 kbar, and 3 kbar as a function of temperature under magnetic field of 0.5 T. The uniaxial pressure and magnetic field are applied parallel to [001]. PM, AFQ, and AFM denote paramagnetic phase, antiferroquadrupolar phase, and antiferromagnetic phases, respectively. The positions where the letters are placed show approximately the temperature regions of the phases.

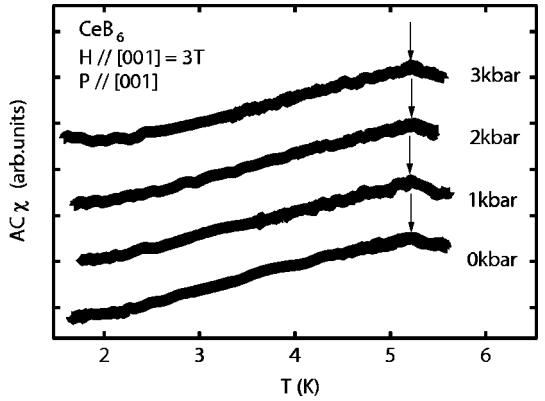

FIG. 4. ac susceptibility of CeB_6 at uniaxial pressures 0 kbar, 1 kbar, 2 kbar, and 3 kbar as a function of temperature under magnetic field of 3 T. The uniaxial pressure and magnetic field are applied parallel to [001]. The zeros of the data points at each pressures are shifted to each other for clarity of presentation. The arrows indicate the positions of peak from which the antiferroquadrupolar transition temperatures have been determined.

Figure 3 shows the ac susceptibility at 0.5 T or in phases I, IIB, and III. It is noted that the curve forms are qualitatively the same under ambient and uniaxial pressures. We have plotted the shoulder and the inflection point of the curve as the right- and left-hand ends of the error bar, respectively. Figure 4 shows the ac susceptibility as a function of temperature at 3 T or in phases I and II. The curve forms are nearly the same for all pressures. It can be also clearly seen that $T_Q(H)$ does not change with pressure within the experimental error of 10 mK.

Next we describe the ac susceptibility measurements at a constant temperature as a function of magnetic field. Figure 5 shows a typical ac susceptibility curve of 0 kbar at 0.12 K in phases III″, III, III′, and II. With increasing field the susceptibility is nearly constant at low fields. Then it makes a broad hump, a sharp peak, and a shoulder, successively. Hereafter, we denote the magnetic fields corresponding to the

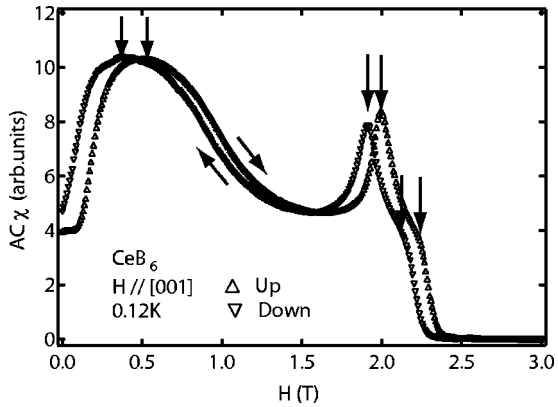

FIG. 5. ac susceptibility of CeB_6 as a function of magnetic field at 0.12 K. The magnetic field is applied parallel to [001]. The triangle symbols for up and down indicate that the data were taken with increasing and decreasing fields, respectively. The vertical arrows show the positions from which the transition fields H_1, H_2, and H_3 have been determined.

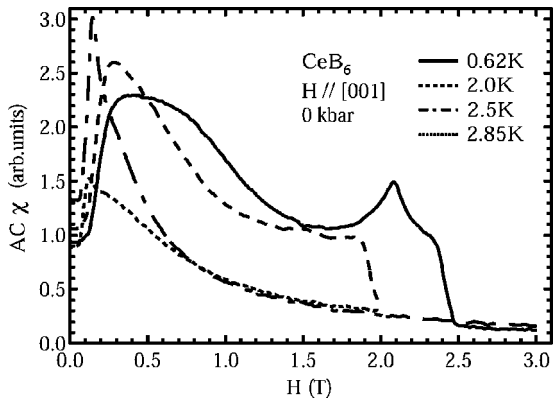

FIG. 6. ac susceptibility of CeB_6 at 0 kbar as a function of magnetic field at temperatures 0.62 K, 2.0 K, 2.5 K, and 2.85 K. The magnetic field is applied parallel to [001].

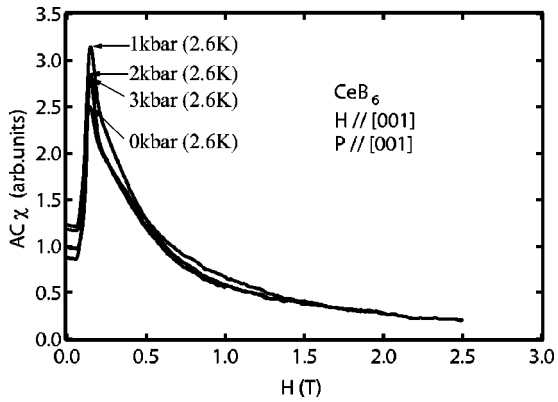

FIG. 8. ac susceptibility of CeB_6 at uniaxial pressures 0 kbar, 1 kbar, 2 kbar, and 3 kbar as a function of magnetic field at about 2.6 K.

top of the hump, the peak, and the shoulder as H_1, H_2, and H_3, respectively. They are defined as the transition fields between phases III″ and III, III and III′, III′ and II, respectively. With decreasing field from above 2.5 T, a similar curve is obtained with clear hysteresis for H_1, H_2, and H_3. At zero field the susceptibility jumps back to the starting value. When we increase the field again, the same curve with the previous curve is obtained.

Figure 6 shows some typical ac susceptibility curves as a function of magnetic field in the AFQ phase (2.85 K and 2.5 K) and the AFM phase (2.0 K and 0.62 K) at ambient pressure. It is noted that in the both phases the susceptibility is nearly constant at low fields and increases steeply approximately at the same field. The peak field in the AFQ phase is defined as the transition field between phases IIA and IIB. The transition shows a hysteresis behavior similar to those of H_1. As noted from the transition fields in the AFQ and AFM phases of Fig. 1, phases IIA and III″ seem to be closely related with each other.

Figure 7 shows the ac susceptibility as a function of field at pressures 0 kbar, 1 kbar, 2 kbar, and 3 kbar at about 0.12 K or in AFM and AFQ phases. With application of 1 kbar, the behavior of ac susceptibility changes considerably at low

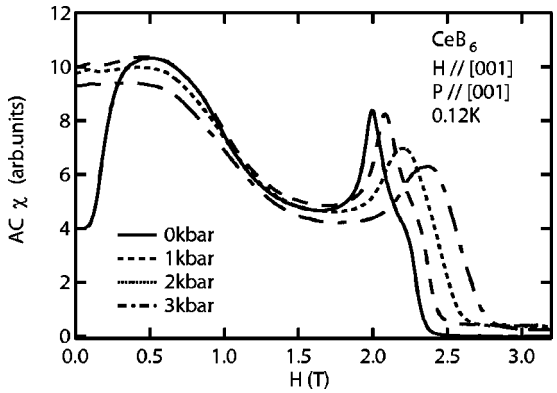

FIG. 7. ac susceptibility of CeB_6 at uniaxial pressures 0 kbar, 1 kbar, 2 kbar, and 3 kbar as a function of magnetic field at 0.12 K. The uniaxial pressure and magnetic field are applied parallel to [001].

fields from that of 0 kbar. This behavior corresponds to the behavior shown in Fig. 2. With further application of pressure, the curve form at low fields does not change further and finally the peak of the hump becomes indistinguishable. This may imply that the difference between phases III″ and III becomes smaller or nothing with application of uniaxial pressure. As long as the peak of the hump is identified, it is plotted in the phase diagram in Fig. 1. As discussed later, the small remnant peak could be due to a small inhomogeneity of strain. The peak and shoulder at H_2 and H_3 shift to higher fields and become broader, and then the shoulder becomes difficult to identify. The dotted lines for H_2 in Fig. 1 are guides to the eye and that for H_3 in Fig. 1 is drawn by assuming the shoulder, if any, sits in the middle between the peak for H_3 and the field where the ac susceptibility becomes approximately constant.

Figure 8 shows the ac susceptibility as a function of magnetic field at about 2.6 K. The sharp increase of susceptibility at ambient pressure corresponds to the phase IIA–phase IIB transition. It is also noted that the susceptibility increases steeply at the phase boundary for all pressures, i.e., the boundary for phase IIB is clearly observed under uniaxial pressures as well as that in the temperature sweep (Fig. 4). This observation is in contrast to the observation that the boundary between phases III″ and III and that between phase I and phase IIA become obscure with application of 1 kbar (Figs. 2 and 7). This point will be discussed in Sec. IV B. The phase boundary for phase IIB does not change appreciably at lower temperatures such as 2.6 K, but slightly increases with pressure at higher temperatures as shown in Fig. 1.

To summarize the result briefly, the uniaxial pressure affects the low-field phases IIA and III″ significantly, but does not change $T_Q(H)$ for phase IIB. $T_N(H)$ for phase III, H_2, and H_3 increase with uniaxial pressure.

B. The dHvA effect

The dHvA effect of CeB_6 has been studied by a number of groups.[14–20] The Fermi surface is quite similar to that of LaB_6, indicating that the *f* electrons of CeB_6 are well localized. There are ellipsoidal electron Fermi surfaces at the *X*

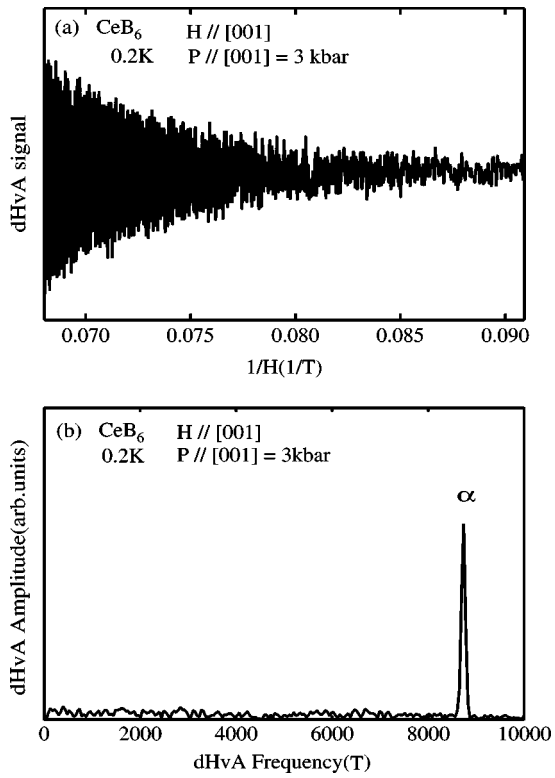

FIG. 9. (a) α_3 dHvA oscillations at 3 kbar presented as a function of inverse field. The uniaxial pressure and magnetic field are applied parallel to [001]. (b) Fourier spectrum of the oscillation in (a).

points which are connected by necks extending in the $\langle 110 \rangle$ directions. These are the main Fermi surfaces of CeB_6. When a field is applied parallel to the [001] direction, the α_3 oscillation arises from this Fermi surface. There are also lower-frequency oscillations ρ, γ, and ϵ. The first and the latter two are attributed to small electron pockets at the neck position and to holelike orbits circulating inside the multiply connected Fermi surface, respectively. We have studied the pressure effect of the α_3 oscillation. The amplitudes of other

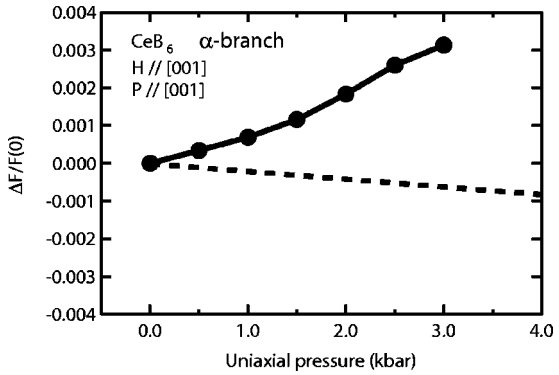

FIG. 10. Relative change of frequency $[F(P)-F(0)]/F(0)$ of the α_3 oscillation as a function of uniaxial pressure, where $F(0)$ and $F(P)$ denote the frequencies at 0 kbar and under pressure, respectively. The uniaxial pressure and magnetic field are applied parallel to [001]. The broken line denotes the frequency change expected from the change in the reciprocal space.

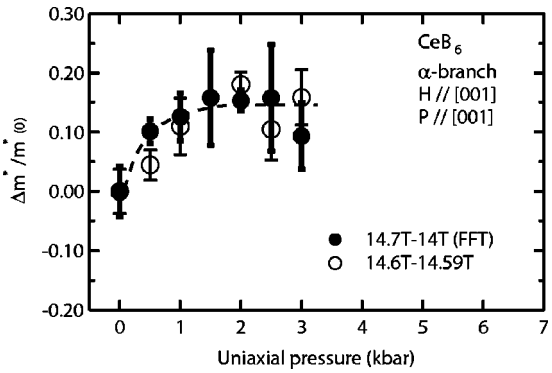

FIG. 11. Relative change of effective mass $[m^*(P)-m^*(0)]/m^*(0)$ for the α_3 oscillation as a function of uniaxial pressure, where $m^*(0)$ and $m^*(P)$ denote the effective masses at 0 kbar and under pressure, respectively. The uniaxial pressure and magnetic field are applied parallel to [001]. The closed and open circles are the data obtained from the FFT analysis and the peak to peak amplitude of the oscillation, respectively. The broken line is a guide to the eye.

oscillations are too small to study their effective masses and frequencies under uniaxial pressures.

Figures 9(a) and 9(b) show the dHvA signal under uniaxial pressure of 3 kbar and its Fourier spectrum. Figure 10 shows the relative frequency change $\Delta F/F(0)=[F(P)-F(0)]/F(0)$ of α_3 as a function of pressure. The frequency change is determined by the phase-shift analysis of the dHvA oscillation around 14.6 T. The dotted line shows the frequency change expected from the change of the reciprocal space, which corresponds to the expansion of the real-space area, perpendicular to the direction of the uniaxial pressure. For the calculation of the broken line, we have used the value of 6.2×10^{-4}/kbar (Ref. 2) for the compressibility and assumed the value of 0.25 for the Poisson ratio. Therefore, the dotted line is a semiquantitative guide for the comparison with the experimental result. Although the dHvA frequency is expected to decrease with uniaxial pressure, the experimental frequency increases with pressure. The magnitude of the frequency change is also much larger than expected.

Figure 11 shows the relative change of the effective mass as a function of pressure. Although the error for the mass measurements is large, it can be seen that the effective mass increases steeply at low pressures and then stays approximately constant at higher pressures. The initial increasing rate is comparable to or more than those observed in the most pressure sensitive heavy fermion compound $CeRu_2Si_2$.[21]

IV. DISCUSSION

A. Comparison with hydrostatic pressure effect

1. Magnetic phase diagram

The hydrostatic pressure effect on T_Q, T_N, and H_n or the phase diagram has been studied by various groups.[2–5] T_Q increases very slightly with pressure (7.67×10^{-3}K/kbar [at 1 kOe for $H//[110]$ (Ref. 5)] or 9×10^{-3}K/kbar (Ref. 2)). The increase is reported to depend on magnetic field and is

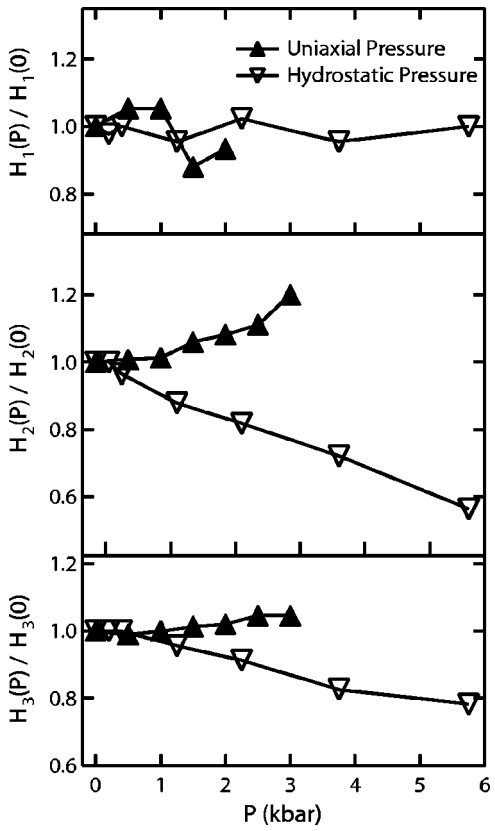

FIG. 12. Transition fields H_1, H_2, and H_3 as a function of pressure. The closed and open triangles denote the data points for uniaxial and hydrostatic pressures, respectively. The data points are normalized with respect to the values at 0 kbar $H_1(0)$, $H_2(0)$, and $H_3(0)$. The uniaxial pressure and magnetic field are applied parallel to [001].

larger at higher magnetic fields.[3,5] On the other hand, Brandt *et al.*[2] shows that the increasing rate does not depend appreciably on magnetic field. It is difficult to tell whether T_Q increases or decreases with uniaxial pressure from the present experiment, but the changing rate is comparable to or smaller than that with hydrostatic pressure.

T_N decreases with hydrostatic pressure and the decreasing rate is -0.039 K/kbar (Ref. 2) or $[T_N(P)-T_N(0)]/T_N(0)$ is -1.6×10^{-2}/kbar. On the other hand, the increasing rate with uniaxial pressure is between 0.05 K/kbar and 0.06 K/kbar or $[T_N(P)-T_N(0)]/T(0)$ is $(4-6)\times10^{-2}$/kbar. It is also noted that the changing rate of T_N is by one order of magnitude smaller than those recently reported for such compounds where hydrostatic pressure can drive T_N to zero,[22] although the compressibility of CeB_6 is comparable to the ordinary alloys or compounds.

The behavior of the ac susceptibility in the AFM state is also different. Under hydrostatic pressure the curve forms of the ac susceptibility shown in the AFM phase (Fig. 2) do not change qualitatively from that at ambient pressure and the transition fields H_1, H_2, and H_3 can be clearly defined under hydrostatic pressures. Figure 12 shows the H_1, H_2, and H_3 at low temperatures of about 100 mK as a function of uniaxial and hydrostatic pressures. The data for the hydrostatic pressure are reproduced from the previous

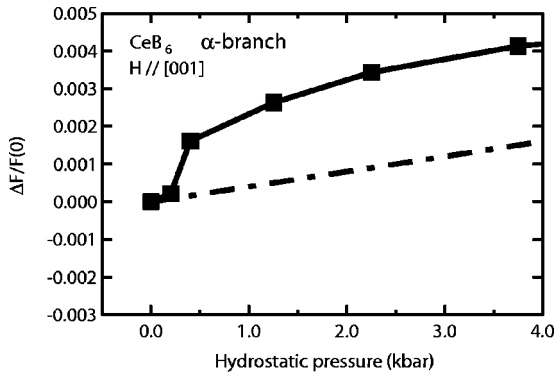

FIG. 13. Relative change of frequency $[F(P)-F(0)]/F(0)$ for the α_3 oscillation as a function of hydrostatic pressure, where $F(0)$ and $F(P)$ denote the frequencies at 0 kbar and under pressure, respectively. The magnetic field is applied parallel to [001]. The dotted-broken line denotes the frequency change expected from the area change in the reciprocal space.

measurements.[6] The relative change $[H_n(P)]/H_n(0)$ is shown instead of H_n itself. The large scatter of the H_1 data for the uniaxial pressure is mostly due to the difficulty to determine the peak position. On the other hand, H_1 for hydrostatic pressure can be clearly defined and does not change with hydrostatic pressure whereas H_2 and H_3 decrease with hydrostatic pressure. The changing rates of H_2 and H_3 are much smaller for uniaxial pressure than for hydrostatic pressure. Since H_3 for uniaxial pressure is difficult to define as described above for Fig. 7, we compare the changing rate of H_2. The decreasing rate for hydrostatic pressure is -0.17 T/kbar or $[H_n(P)-H_n(0)]/H_n(0)$ is -9×10^{-2}/kbar. On the other hand, H_2 does not increase linearly with uniaxial pressure and the increasing rate at low pressures is between 0.032 T/kbar and 0.076 T/kbar, or $[H_n(P)-H_n(0)]/H_n(0)$ is between 1.7×10^{-2} and 4.0×10^{-2}. It is noted that $[H_n(P)-H_n(0)]/H_n(0)$ is by one order of magnitude larger than $[T_N(P)-T_N(0)]/T_N(0)$ for hydrostatic pressure but they are comparable for uniaxial pressure.

2. dHvA effect

Figure 13 shows the relative frequency change as a function of hydrostatic pressure determined from the phase-shift analysis. The dotted-broken line indicates the frequency change expected from the decrease of the volume change or the expansion of the reciprocal space. The frequency increases rapidly at lower pressures and then changes almost linearly with pressure. The initial increasing rate at low pressures is comparable to that of the heavy fermion compound $CeRu_2Si_2$,[21] or even larger than that, if we compare the rate with that of dHvA frequency with similar size. On the other hand, the increasing rate at high pressures is comparable to that of the dotted-broken line. Figure 14 shows the relative change of the effective mass as a function of hydrostatic pressure. The data were reproduced from Fig. 2 of our previous paper[6] to show the relative change of the effective mass. The effective mass decreases rapidly at lower pressures and then becomes approximately constant at higher

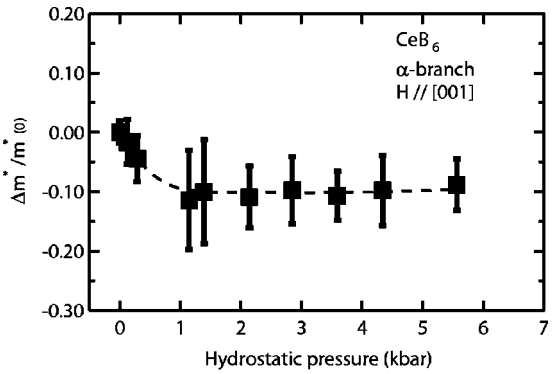

FIG. 14. Relative change of effective mass $[m^*(P) - m^*(0)]/m^*(0)$ for the α_3 oscillation as a function of hydrostatic pressure, where $m^*(0)$ and $m^*(P)$ denote the frequencies at 0 kbar and under pressure, respectively. The magnetic field is applied parallel to [001]. The broken line is a guide to the eye.

pressures. This behavior is also qualitatively similar to that under uniaxial pressure in the sense that the effective mass changes rapidly at low pressures, but the direction of the change is opposite to that under uniaxial pressures.

Let us stress that the nonlinear behavior of the dHvA results under uniaxial and hydrostatic pressures is intrinsic from the following reasons.

(1) We have studied the dHvA effect under hydrostatic and uniaxial pressures in a number of compounds[10,11,21,23–27] by using almost the same experimental setting and observed linear change of the frequency and effective masses. Sometimes the effect is not linear with respect to applied pressure for a few dHvA frequencies, but the effect is linear for the other frequencies in the same compound indicating that the nonlinear behavior is intrinsic.

(2) Although T_N, H_n, and T_Q are measured in the same experimental setting with the dHvA measurements, the behavior is not qualitatively the same as those found for the effective mass or the frequency.

It is not clear why the effective mass or frequency behaves like that at present stage. In the later discussions, we analyze only the behavior at low pressures assuming that the quantities change linearly with pressure.

B. Low-field phases

Here we will discuss the low-field phases IIA and III″. The neutron experiment with fields along other directions indicates that the lowest-field state is a domain state.[13] Therefore, it is also possible that the phases IIA and III″ in this direction are domain states. We have performed zero-field cooled and field cooled experiments in phases IIA and IIB and found no difference in the ac susceptibility between them as a function of temperature. We also performed ac susceptibility measurements in phases IIA and IIB with increasing the field from zero to across the boundary, and then with decreasing the field to zero. We repeated this process and found no difference in the ac susceptibility between the first and the second run. We think that the phase IIA is not likely to be a domain state but a phase. The magnetic phase diagram (Fig. 1) and ac susceptibility as a function of field (Fig. 6) suggest that phases IIA and III″ are closely related with each other. We have repeated ac susceptibility measurements in phases III″, III, III′, and II by increasing, decreasing, and again increasing the field from zero beyond the phase boundary and found no difference between the first and the second field sweeps from zero. Therefore, phase III″ is also unlikely to be a domain state.

The temperature dependence of susceptibility (Fig. 2) has a curve form similar to that of the parallel susceptibility of an antiferromagnet in the sense that the curve has a peak structure. However, the susceptibility does not decrease much with decreasing temperature suggesting that the magnetic moments are not parallel to the field direction. With application of a small uniaxial pressure, the curve form becomes similar to that of the perpendicular susceptibility of an antiferromagnet. The magnetic moments in phase III lie in the x-y plane[28] and therefore the curve form is consistent. Since the difference in the susceptibility between phases III and III″ becomes small (Fig. 7) with application of uniaxial pressure, it is very likely that the phase III″ disappears with application of a small uniaxial pressure.

Next we will argue that phase IIA is also likely to disappear with application of a small uniaxial pressure. The quadrupolar order in phase IIB is most likely to be the O_{xy} type which is consistent with the magnetic structure in phase III.[29] Then, since no magnetic moment is observed in phase II at zero magnetic field at ambient pressure,[13,28] phase IIA could have a different quadrupolar order from that of phase IIB. Figures 4 and 8 show that phase IIB is not significantly affected by the uniaxial pressure, while Fig. 2 shows that phase IIA is significantly affected. Moreover, the susceptibility change between phases I and IIA becomes very small under uniaxial pressure. If the weak remnant changes under uniaxial pressures are due to inhomogeneous strain in the sample, the present results indicate that the susceptibility changes smoothly across T_Q under uniaxial pressures. This implies that, with application of a small uniaxial pressure the phase IIA disappears, or that although the phase IIA exists T_Q in phase IIA becomes almost independent of magnetic-field strength as the Ehrenfest's relation tells us. Since the magnetic structure of phase III″, which appears to be closely related with the quadrupolar state in phase IIA, disappears under uniaxial pressures, we suspect that the phase IIA disappears together with phase III″. Moreover, if we could define T_N as the peak position of the susceptibility curve, a careful examination of Fig. 2 indicates that T_N at 1 kbar is smaller than that at ambient pressure and then T_N increases with increasing uniaxial pressure. In other words, the transitions under uniaxial pressures could be qualitatively different from that at ambient pressure, i.e., the phase IIA–phase III″ transition at ambient pressure could have changed to the phase I–phase III transition under uniaxial pressures. Further studies are necessary to clarify the nature of states IIA and III″, which could be closely related with the mysterious properties of $Ce_xLa_{1-x}B_6$.

In the following discussions, we use $T_N(H)$ at 0.5 T as the transition temperature from AFQ phase to AFM phase which

corresponds to the transition from IIB to III. In other words, we discuss the properties under the quadrupolar order of O_{xy} type.

C. Implications of uniaxial and hydrostatic pressure effects

Finally, we will discuss the implications of the qualitatively different effects between hydrostatic and uniaxial pressures. Before we go into the discussion, let us consider how the pressure affects the system with quadrupolar order. We assign the z direction to the [001] directions which is parallel to the magnetic field and to the direction of uniaxial stress. Since both, the hydrostatic pressure and the uniaxial pressure along the z axis do not produce ϵ_{xy}-type strain, it is not necessary to take the direct coupling between the quadrupole and strain into account. In fact, the transition temperature from phase I to phase IIB does not change applicably with uniaxial pressure. When the O_{xy}-type quadrupolar order takes place with fields parallel to the z axis, the direction along the z axis and the directions in the x-y plane are no longer equivalent and consequently the effect of the compression may not be equivalent between the z and in-plane directions. Hydrostatic pressure gives rise to compression along z direction as well as along the in-plane directions. Therefore, it is difficult to distinguish the effects of the z and in-plane compressions independently from hydrostatic pressure experiment. On the other hand, the uniaxial pressure gives rises to compression along z direction and expansion along the in-plane directions. In the following by comparing the hydrostatic and uniaxial pressure effects, we will make a qualitative estimate of the effects of the compressions along the axis and in the x-y plane.

In the present experiment the effect of uniaxial pressure on T_Q is found to be very small. It is also shown that T_Q increases very slightly[3,5] or is constant[2] with increasing hydrostatic pressure. If a negative hydrostatic pressure or an expansion gives an opposite effect to that of a positive hydrostatic pressure or a compression, it is likely that the effects of compressions along the axis and the expansion in the x-y plane are canceled to give a small effect on T_Q.

The dHvA frequency increases with hydrostatic pressure and also with uniaxial pressure. The interpretation of these changes may not be simple. The experiment was performed in phase IIB under high magnetic fields and therefore the z direction and the x, y directions are not equivalent. Consequently, the ellipsoidal Fermi surface at the X_z point is not equivalent to those at the X_x and X_y points. The change of Fermi surface at the X_z point with pressure, particularly with uniaxial pressure, is different from those at the X_x and X_y points. Since the number of the conduction electrons is not expected to change with pressure, the change of one Fermi surface affects the changes of the other Fermi surfaces. Therefore, the observed change of the dHvA frequency, i.e., the extremal cross-sectional area of the Fermi surface at the X_z point is a complicated combined effect. Moreover, when a large change of magnetization is induced with uniaxial pressure, it is necessary to measure the frequency change as a function of B and the observed frequency change as a function of H does not exactly correspond to the Fermi-surface change. Since the magnetization change under uniaxial pressures at high fields has not been measured, we will not discuss the frequency change at the present stage.

TABLE I. Relative changes of T_N, H_2, and m^* under hydrostatic and uniaxial pressures. The values are given in units of kbar^{-1}.

	Hydrostatic pressure	Uniaxial pressure
$\Delta T_N/T_N(0)$	-1.6×10^{-2}	$(4-6)\times10^{-2}$
$\Delta H_2/H_2(0)$	-9×10^{-2}	$(1.7-4.0)\times10^{-2}$
$\Delta m^*/m^*(0)$	-0.13	0.15

[a]Reference 2.

In the following analysis we discuss only the changes of T_N, H_2, and m^*.

The changing rates for T_N, H_2, and m^* with hydrostatic and uniaxial pressures are summarized in Table I. It is noted that the effect of uniaxial pressure is opposite to that of hydrostatic pressure, i.e., the values decrease with hydrostatic pressure but increase with uniaxial pressure. The magnitudes of the changes of m^* and T_N due to uniaxial pressure are comparable to or larger than those due to hydrostatic pressure. On the other hand, the changing rate of H_2 due to the hydrostatic pressure is larger than that due to uniaxial pressure. Since that of T_N is comparable or smaller than that due to uniaxial pressure, we expect that the changing rate of H_2 due to hydrostatic pressure is comparable to or smaller than that due to uniaxial pressure.

To understand the implications of these observations a little more quantitatively, we make an analysis of the results making the following assumptions.

As long as the pressure or the lattice change is small:

(a) A negative pressure gives the same but reversed effect on the physical properties and electronic structure to that of positive pressure. For example when the hydrostatic pressure P_h decreases the effective mass by an amount of Δm^*, then the negative pressure $-P_h$ increases the effective mass by the same amount.

(b) Compressibility is isotopic. This is not self-consistent with the following result of very anisotropic effect of compression. But this assumption would be useful to reveal the anisotropic behavior.

(c) The quantity changes linearly with applied pressure, irrespective of that the pressure is positive and negative.

(d) The Poisson ratio is assumed to be 0.25.

Case 1. First we estimate the effect of the compression along the axis. A negative hydrostatic pressure $-P_{h_1}$ expands the lattice constant a by Δa. $\Delta a/a$ is given by $P_{h_1}/3K$, where K is the compressibility. A uniaxial pressure P_{u_1} along the z axis expands the lattice in the x-y plane directions by $\Delta a'$ and compresses the lattice by $\Delta a''$ along the axis. $\Delta a'/a$ and $\Delta a''/a$ are given by $\mu P_{u_1}/[3K(1-2\mu)]$ and $P_{u_1}/[3K(1-2\mu)]$, respectively. We assume that Δa and $\Delta a'$ are the same. Then, by comparing these two states under hydrostatic and uniaxial pressures, we may estimate the effect of the compression from $a+\Delta a$ to $a-\Delta a''$ along the z axis at the state with lattice constant a

TABLE II. Estimated changes of T_N, H_2, and m^* when the sample is compressed along the z axis or in the x-y plane (in-plane). The signs + and − denote that the quantity increases and decreases with compression, respectively. In-plane/axis denotes the relative ratio of the magnitudes in the changes due to the compressions in the plane and along the axis.

	ΔT_N	ΔH_2	Δm^*
In-plane	−	−	−
Axis	+	−	+
In-plane/axis	4–5	5–32	5

$+\Delta a$. Since $\Delta a = \Delta a'$ and $2\mu = 0.5$, then $P_{u_1} = 2P_{h_1}$. That is, the effect of the compression can be estimated from the difference of the quantities at the state with uniaxial pressure $P_{u_1} = 2P_{h_1}$ and that with hydrostatic pressure $-P_{h_1}$. The lattice change by the compression is $(\Delta a + \Delta a'')/a$ which is given by $P_{h_1}(1+1/\mu)/3K$.

Case 2. Next we estimate the effect of the compression in the x-y plane. A positive pressure P_{h_2} compresses the lattice by Δa and $\Delta a/a$ is given by $P_{h_2}/3K$. A uniaxial compression P_{u_2} along the z direction compresses the lattice by $\Delta a'$ and $\Delta a'/a$ is given by $P_{u_2}/[3K(1-2\mu)]$. It expands the lattice in the x-y plane by $\Delta a''$ and $\Delta a''/a$ is given by $\mu P_{u_2}/[3K(1-2\mu)]$. We assume that Δa and $\Delta a'$ are the same. Then, by comparing the two states under hydrostatic and uniaxial pressures we may estimate the effect of the compression in the x-y plane from $a+\Delta a''$ to $a-\Delta a$ at the state with the lattice constant $a-\Delta a$. Since $\Delta a = \Delta a'$, $P_{u_2} = (1-2\mu)P_{h_2} = 0.5P_{h_2}$. That is, the effect of the compression in the x-y plane is given by the difference of the quantities at the state with uniaxial pressure $P_{u_2} = 0.5P_{h_2}$ and that with hydrostatic pressure P_{h_2}. The lattice change in the plane due to the compression is $(\Delta a + \Delta a'')/a$ which is given by $P_{h_2}(1+\mu)/3K$.

Now, let us compare the effects of the compressions along the z axis and in-plane directions. It would be reasonable to compare the two effects when the compression along the axis and those in the x-y plane give the same volume change. The volume changes $\Delta V/V$ in cases 1 and 2 are given by $P_{h_1}(1+1/\mu)/3K$ and $2P_{h_2}(1+\mu)/3K$, respectively. Then from this condition the relation between P_{h_1} and P_{h_2} is calculated to be $P_{h_1} = 2(1+\mu)P_{h_2}/(1+1/\mu)$ or $P_{h_1} = 0.5P_{h_2}$. That is, when we compare the two effects, we have to compare the change from $-P_{h_1}$ to P_{u_1} $(=2P_{h_1})$ with that from P_{u_2} $(=0.5P_{h_2} = P_{h_1})$ to P_{h_2} $(=2P_{h_1})$.

Table II summarizes whether the quantity increases or decreases and the ratios of the changes associated with compressions along the z axis and in the x-y plane. T_N and m^* increase with the compression along the axis and decrease with the compression in the plane. On the other hand, H_2 decreases both with the compression along the axis and in the plane. This is a consequence from the peculiar features of the experimental results for H_2 which is different from those of T_N and m^* mentioned above. This result may imply that an interaction which competes with the antiferromagnetic interaction is present under magnetic fields and the magnitude of the interaction increases with compressions both along the z axis and in the x-y plane.

The present analysis strongly suggests that the pressure effect is very anisotropic depending on whether the compression is along the z axis or in the x-y plane. Since all the quantities are closely related with the interaction among the f electrons of neighboring sites or the interaction between the f electron and the conduction electrons, it is very plausible that the anisotropic effect arises from the anisotropic f electron state. The difference between the z direction and the in-plane directions is consistent with the quadrupolar order of O_{xy} type. The anisotropic pressure effect also implies that the electronic structure itself or the interactions related with the electronic structure are anisotropic in the ordered sate of quadrupole. However, it is difficult to understand in a straightforward manner why the effect is reversed between the compressions along the z axis and in the x-y plane.

V. SUMMARY AND CONCLUSION

We have investigated the magnetic phase diagram and the electronic structure of CeB_6 under uniaxial pressure. The low-field phases IIA and III″ seem to be closely related with each other at ambient pressure and are very likely to disappear with application of a small uniaxial pressure. On the other hand, T_Q for phase IIB does not change within the experimental error with application of uniaxial pressure up to 3 kbar. $T_N(H)$ for phase III, H_2, and H_3 increase with uniaxial pressure. The dHvA frequency of the α_3 oscillation increases with uniaxial pressure, although it is expected to decrease reflecting the area change in the reciprocal space. The effective mass increases rapidly with uniaxial pressure at low pressures and stays approximately constant at high pressures. The changes of T_N, H_n, and m^* due to uniaxial pressure are qualitatively opposite to those found for hydrostatic pressure. By analyzing the uniaxial and hydrostatic pressure effects together, we have shown that the effects of the compressions along the z axis and in the x-y plane are possibly very different in the ordered state of O_{xy}-type quadrupoles.

ACKNOWLEDGMENTS

We thank Professor T. Goto, Professor H. Harima, and Dr. S. Nakamura for useful discussions and comments on our data. We also thank M. Suzuki and M. Kikuchi for technical support. This work was supported by a Grant-in-Aid for Scientific Research from Mext Japan.

*Electronic address: aokih@mail.clts.tohku.ac.jp

[1] S. Doniach, Physica B & C **91**, 231 (1977).
[2] N.B. Brandt, V.V. Moschalkov, S.N. Pashkevich, M.G. Vybornov, M.V. Semennov, T.N. Kolobyanina, E.S. Konovalova, and Yu.B. Paderno, Solid State Commun. **56**, 937 (1985).
[3] T.C. Kobayashi, K. Hashimoto, S. Eda, K. Shimizu, K. Amaya, and Y. Onuki, Physica B **281&282**, 553 (2000).
[4] S. Sullow, V. Trappe, A. Eichler, and K. Winzer, J. Phys.: Condens. Matter **6**, 10 121 (1994).
[5] Y. Uwatoko, K. Kosaka, M. Sera, and S. Kunii, Physica B **281&282**, 555 (2000).
[6] C.J. Haworth, H. Aoki, M. Takashita, T. Terashima, and T. Matsumoto, J. Magn. Magn. Mater. **177-181**, 371 (1998).
[7] T. Yamamizu, M. Nakayama, N. Kimura, T. Komatsubara, and H. Aoki, J. Magn. Magn. Mater. **226-230**, 155 (2001).
[8] T. Yamamizu, M. Nakayama, N. Kimura, T. Komatsubara, and H. Aoki, Physica B **226-230**, 155 (2001).
[9] H. Nakao, K. Magishi, Y. Watanabe, Y. Murakami, K. Kayama, K. Hirota, Y. Endoh, and S. Kunii, J. Phys. Soc. Jpn. **70**, 1857 (2001).
[10] M. Takashita, H. Aoki, T. Matsumoto, C.J. Haworth, T. Terashima, A. Uesawa, and T. Suzuki, Phys. Rev. Lett. **78**, 1948 (1997).
[11] M. Takashita, H. Aoki, C.J. Haworth, T. Matsumoto, T. Terashima, S. Uji, C. Terakura, T. Miura, A. Uesawa, and T. Suzuki, J. Phys. Soc. Jpn. **67**, 3859 (1998).
[12] S. Nakamura, T. Goto, and S. Kunii, J. Phys. Soc. Jpn. **64**, 3941 (1995).
[13] P. Burlet, J. Rossat-Mignod, J.M. Effantin, T. Kasuya, S. Kunii, and T. Komatsubara, J. Appl. Phys. **53**, 2149 (1982).
[14] A.P.J. van Deursen, Z. Fisk, and A.R. de Vroomen, Solid State Commun. **44**, 609 (1982).
[15] T. Suzuki, T. Goto, S. Sakatsume, A. Tamaki, S. Kunii, and T. Fujiwara, Jpn. J. Appl. Phys., Part 1 **26**, 511 (1987).
[16] Y. Onuki, T. Komatsubara, P.H. Reinders, and M. Springford, J. Phys. Soc. Jpn. **58**, 3698 (1989).
[17] W. Joss, J.M. van Ruitenbeek, G.W. Crabtree, J.L. Tholence, A.P.J. van Deursen, and Z. Fisk, Phys. Rev. Lett. **59**, 1609 (1987).
[18] N. Harrison, P. Meeson, P-A. Probst, and M. Springford, J. Phys.: Condens. Matter **5**, 7435 (1993).
[19] N. Harrison, D.W. Hall, R.G. Goodrich, J.J. Vuillemin, and Z. Fisk, Phys. Rev. Lett. **81**, 870 (1998).
[20] R.G. Goodrich, N. Harrison, A. Teklu, D. Young, and Z. Fisk, Phys. Rev. Lett. **82**, 3669 (1999).
[21] H. Aoki, M. Takashita, N. Kimura, T. Terashima, S. Uji, T. Matsumoto, and Y. Onuki, J. Phys. Soc. Jpn. **70**, 774 (2001).
[22] P. Coleman, C. Pepin, Qimiao Si, and R. Ramazushvii, J. Phys.: Condens. Matter **13**, R723 (2001).
[23] H. Aoki, M. Takashita, C.J. Haworth, T. Matsumoto, T. Terashima, S. Uji, C. Terakura, A. Uezawa, and T. Suzuki, J. Magn. Magn. Mater. **177-181**, 371 (1998); **56**, 937 (1985).
[24] M. Takashita, H. Aoki, C.J. Haworth, T. Matsumoto, C. Terakura, S. Uji, T. Miura, K. Maezawa, R. Settai, and Y. Onuki, J. Magn. Magn. Mater. **177-181**, 417 (1998).
[25] M. Takashita, H. Aoki, T. Miura, C. Terakura, S. Uji, T. Matsumoto, K. Maezawa, R. Settai, and Y. Onuki, Physica B **259-261**, 1093 (1999).
[26] M. Takashita, H. Aoki, T. Terashima, C. Terakura, T. Matsumoto, T. Nishigaki, H. Sugawara, Y. Aoki, and H. Sato, Physica B **281&282**, 738 (2000).
[27] T. Terashima, T. Matsumoto, C. Terakura, S. Uji, N. Kimura, M. Endo, T. Komatsubara, and H. Aoki, Phys. Rev. Lett. **87**, 166401 (2001).
[28] J.M. Efantin, J. Rossat-Mignod, P. Burlet, H. Bartholin, S. Kunii, and T. Kasuya, J. Magn. Magn. Mater. **47-48**, 145 (1985).
[29] W.A.C. Erkenlens, L.P. Regnault, P. Burlet, J. Rossat-Mignod, S. Kunii, and T. Kasuya, J. Magn. Magn. Mater. **63&64**, 61 (1987).